Histol Histopathol (2020) 35: 1363-1377

http://www.hh.um.es

Histology and Histopathology
From Cell Biology to Tissue Engineering

Paracervical ganglion in the female pig during prenatal development: morphology and immunohistochemical characteristics

Amelia Franke-Radowiecka

Department of Animal Anatomy, Faculty of Veterinary Medicine, University of Warmia and Mazury, Olsztyn, Poland

Summary. The present study investigated the development of the paracervical ganglion in 5-, 7- and 10-week-old porcine foetuses using double labelling immunofluorescence method. In 5-week-old foetuses single PGP-positive perikarya were visible only along the mesonephric ducts. They contained DβH or VAChT, and nerve fibres usually were PGP/VAChT-positive. The perikarya were mainly oval. In 7-week-old foetuses, a compact group of PGP-positive neurons (3144±213) was visible on both sides and externally to the uterovaginal canal mesenchyme of paramesonephric ducts. Nerve cell bodies contained only DβH (36.40±1.63%) or VAChT (17.31±1.13%). In the 10-week-old foetuses, the compact group of PGP-positive neurons divided into several large and many small clusters of nerve cells and also became more expanded along the whole uterovaginal canal mesenchyme reaching the initial part of the uterine canal of the paramesonephric duct. The number of neurons located in these neuronal structures increased to 4121±259. Immunohistochemistry revealed that PGP-positive nerve cell bodies contained DβH (40.26±0,73%) and VAChT (30.73±1.34%) and were also immunoreactive for NPY (33.24±1,27%), SOM (23.6±0,44%) or VIP (22.9±1,13%). Other substances studied (GAL, NOS, CGRP, SP) were not determined at this stage of the development. In this study, for the first time, the morphology of PCG formation in the porcine foetus has been described in three stages of development. Dynamic changes in the number of neurons and their sizes were also noted, as well as the changes in immunochistochemical coding of maturing neurons.

Key words: Paracervical ganglion, Peptides, Prenatal development, Pig

Introduction

Pelvic ganglia are important autonomic peripheral nerve centres providing postganglionic nerve supply to the caudal part of the digestive tract and urogenital organs (Kanerval et al., 1972; Mitchell and Ahmed, 1992; Mitchell et al., 1993; Botti et al., 2009; Ragionieri et al., 2013; Kaleczyc et al., 2003, 2020; Pidsudko et al., 2019). These ganglia form large structures as well as smaller nerve cell clusters which were observed in the pelvic area and walls of the pelvic viscera (Nouhouayi and Negulesco, 1983; Mitchell and Ahmed, 1992; Mitchell et al., 1993; Keast, 1999; Kaleczyc et al., 2003, 2020; Pidsudko et al., 2019). Generally, postganglionic axons, originating from pelvic ganglia activate bladder and gut muscles constriction, mediate regulation of the muscle tone of internal genital organs and cause blood vessel relaxation in external genital organs (Mitchell, 1993; Mitchell et al., 1993; Podlasz and Wasowicz, 2008; Botti et al., 2009; Ragionieri et al., 2013; Keast et

Offprint requests to: Amelia Franke-Radowiecka, Department of Animal Anatomy, Faculty of Veterinary Medicine, University of Warmia and Mazury, Oczapowskiego 13, 10-689 Olsztyn, Poland. e-mail: ameliaf@uwm.edu.pl

DOI: 10.14670/HH-18-287

Abbreviations. CGRP, Calcitonin gene related peptide; DβH, Dopamine beta hydroxylase; GAL, Galanin; NCSCs, sacral neural crest-derived progenitor cells; NOS, Nitric Oxide Synthase; NPY, Neuropeptide Y; PGP 9.5, Proteine gene product 9.5; PCG, paracervical ganglion; SOM, somatostatin; SP, Substance P; VIP, Vasoactive Intestinal Peptide; VAChT, Vesicular Acetylcholine Transporter

al., 2015). The greatest part of the female pelvic neuronal plexus structure is the paracervical ganglion (PCG) which is located in the parametrium at the utero-vaginal junction (Bell, 1972; Kanerval, 1972; Kanerval and Teravainen, 1972; Wasowicz et al., 2002; Podlasz and Wasowicz, 2008). In immature and mature animals, PCG neurons are adrenergic or cholinergic but additionally contain many biologically active substances, which proves their wide influence on the functioning of the pelvic organs and their correlation. Previous studies have shown that between the 5th and 10th week of prenatal development in pigs there are dynamic and visible changes in the development of innervation of the internal genital organs (Franke-Radowiecka et al., 2019). It is also known that sacral neural crest-derived progenitor cells (NCSCs) are migratory cells expressing Sox10 which differentiate to form sensory and autonomic innervation for a variety of organs, including the distal hindgut and lower urogenital tract (Kapur, 2000; Britsch et al., 2001; Anderson et al., 2006; Davies, 2009; Wang et al., 2011; Wiese et al., 2012, 2017), TuJ1 or PGP9.5 (Wiese et al., 2017) labelling and have been studied in rodents only (Shakhova and Sommer, 2010; Wiese et al., 2012, 2017). Despite these results, which greatly expanded knowledge regarding migratory pathways, the mechanism of proliferation and differentiation to neurons, glial or other non-neuronal type of cells, e.g. melanocytes (Shakhova and Sommer, 2010; Wiese et al., 2012, 2017), there is a lack of data dealing with the development, topography and chemical coding of foetal PCG neurons in different animal species, including the pig, as a valued breeding animal and increasingly used species in biomedical research (Swindle et al., 2012).

Concerning the above data, the current research aims to trace, for the first time, changes in PCG development in porcine female foetuses. To disclose the dynamics of potential changes, the foetuses were collected at different stages (early, middle and advanced) of gestation.

The results obtained could complement previous studies regarding innervation of internal female genital organs in 5-, 7- and 10-week-old female pig foetuses (Franke-Radowiecka et al., 2019).

Materials and methods

The porcine foetuses were obtained from a slaughterhouse. According to Polish law and EU directive No. 2010/63/EU, the experiments performed in the present study do not require the approval of the Ethics Committee. In this research, 5-week-old (5 litters; 3-4 cm in length; n=19), 7-week-old (4 litters; 7-8 cm in length; n=13) and 10-week-old (3 litters; 13-14 cm in length; n=14) female foetuses were used. The age of the foetuses was marked according to the crown-rump length (CRL) method. CRL sets the distance from the top of the head of the embryo or foetus entering the lower limit of the buttocks (Evans and Sack, 1973).

Tissue preparation and immunohistochemistry

After removing the foetuses from the uterus, the abdominal skin was cut for better penetration of the fixative solution in all collected animals. Foetuses were fixed by immersion in 4% buffered paraformaldehyde (pH 7.4; time incubation 5-, 7-, and 10-week-old foetuses were 1h, 2h, or 4h, respectively), rinsed with phosphate buffer (pH 7.4; overnight, in a refrigerator) and transferred into an 18% buffered sucrose solution (pH 7.4) where they were stored until further processing. The internal genital organs were dissected, then cut transversely or longitudinally on the 12 μm-thick cryostat sections and were processed for single- or double-labelling immunofluorescence as described earlier (Klimczuk et al., 2005; Franke-Radowiecka, 2011; Zalecki, 2012; Franke-Radowiecka et al., 2016, 2019). The sections were labelled using antibodies against PGP, DβH, VAChT, CGRP, SP, NPY, VIP, GAL, and NOS listed in Table 1. After air-drying at room temperature (RT) for 30 min. the sections were pre-incubated with a blocking mixture containing 10% normal horse serum, 1% bovine serum albumin and 0.05% Tween 20 in PBS (1h, RT). They were then incubated with a mixture of appropriate secondary antibodies (listed in Table 1). After rinsing in PBS (3x10 min) the slides were cover-slipped with carbonate-buffered glycerol (pH 8.6).

The omission of primary antisera and their replacement by normal, non-immune sera (rabbit, mouse or rat) was used to investigate the specificity of immunohistochemical labelling. No fluorescence was observed in any of these control stainings, which confirmed the specificity of the staining. The labelled sections were viewed under a Zeiss Axiophot fluorescence microscope equipped with epifluorescence and an appropriate filter set for AlexaFluor 488 and AlexaFluor 555.

Counting of neurons

The total number of PGP-positive neurons in the PCG were counted in every slice (seven-week-old foetuses, neurons were not larger then 11 μm; 5 foetuses) and every second slice (n=5, ten-week-old foetuses, neurons were not larger then 17 μm; 5 foetuses). The neurons with a visible nucleus were only counted on the slice. To determine the percentage (as described earlier, Kaleczyc et al., 2020) of particular neuronal populations, at least 300 neuronal profiles for each combination of antisera were counted. The sections of PCGs were collected from different, representative regions of the ganglia (from its upper, middle and lower one-third). The number of immunolabelled profiles was calculated as a percentage of immunoreactive neurons in regard to all perikarya counted. The obtained data were statistically analysed using the Statistica 13.1 software. To verify the hypotheses, one- and two-factor variance tests and analyses were used (Fisher's test). Moreover, to

evaluate the difference between mean values, Student's t-test and Bonferroni's test were used. The hypotheses were verified at the significance level of α=0.01. All results were expressed as means ± SEM.

PCR, Sex identification

Preliminary sex identification based on morphological observations was confirmed by the PCR technique as described earlier (Franke-Radowiecka et al., 2019). From each 5-week-old foetus, a piece of tail was collected in PCR tubes and preserved in a phosphate-buffered saline (PBS) buffer. To isolate DNA, a modified approach described by Lopez M.E 2012 (A Quick, No-Frills Approach to Mouse Genotyping, Manuel E. Lopez, http://www.bio-protocol.org/e244 Vol 2, Iss 15, Aug 05, 2012) was employed. In all samples, PBS was replaced with 75 µl of 50 mM NaOH, ensuring that the tissues were completely submerged. The samples were then incubated in a thermocycler (T Professional Basic Gradient, Biometra) at 98°C for 45 min to digest the tissues. After incubation, hot, digested tissues were immediately flicked and vortexed, which allowed for complete DNA release. PCR was performed using a Start Warm PCR Master mix (AA Biotechnology) following the manufacturer's protocol on a T Professional Basic Gradient instrument (Biometra). Single PCR reaction included a 1 µL portion of DNA isolation product. Oligonucleotide primers were selected to detect porcine sex by determining the Y (SRY) gene region (F: 5' AAGTCACTCACAGCCCATGAA 3'; R: 5' CCATGGAAGTTCCTGTATCAT 3'). The quality of the sample was checked with the glyceraldehyde 3-phosphate dehydrogenase (GAPDH) reference gene (F: 5' ACATTGTCGCCATCAATG 3', R: 5' ATGCCCAT CACAAACATG 3'). For gel electrophoresis, 2% agarose gel with ethidium bromide (EtBr) was used. Samples in which an SRY-positive band (581 bp product) was detected were recognized as male (A), while samples in which no band was detected were recognized as female (B).

Results

Five-week-old foetuses

During this stage of prenatal development, the paracervical ganglion was not yet visible. Immunohistochemical staining showed that PGP-positive nerve structures ran ventrally from the spinal cord towards the sympathetic chain ganglia to the abdominal cavity (Fig. 1a-d). Single PGP-positive fibres and a few neurons were observed along genital ridges and the mesonephric ducts (Fig. 2a-b; Table 2). These neurons were mainly oval with a large nucleus and a small amount of cytoplasm. The size of these nerve cells was 6-11 µm but most of them were 7-9 µm. Due to the lack of a clearly localized ganglion as well as the inability to determine what the observed nerve cells will innervate, they were not counted in foetuses at the studied developmental stage.

Double-immunohistochemical staining showed that single PGP-positive neurons which were visible along the caudal part of mesonephric ducts were DBH- (Fig 2c,e) or VAChT-positive (Fig. 2d,f). DBH-positive nerve cell bodies were more often noted than VAChT-positive

Table 1. List of primary antisera and secondary reagents used in the study.

Primary antibodies					
Antigen	Clonality	Host	Dilution	Company	Catalog no
Calcitonin gene related peptide (CGRP)	polyclonal	rabbit	1:600	Sigma	C8198
Dopamine beta hydroxylase (DβH)	monoclonal	mouse	1:500	Millipore	MAB308
Dopamine beta hydroxylase (DβH)	polyclonal	rabbit	1:500	Enzo	BML-DZ1020-0050
Galanin (GAL)	polyclonal	rabbit	1:2000	Sigma	AB2233
Nitric Oxide Synthase, Brain (1-181) (NOS)	monoclonal	mouse	1:2000	Sigma	N2280
Neuropeptide Y (NPY)	polyclonal	rabbit	1:5000	Enzo	BML-NZ1233-0025
Neuropeptide Y (NPY)	polyclonal	rat	1:400	Enzo	BML-NZ1115-0025
Protein gene product 9.5 (PGP 9.5)	monoclonal	mouse	1:400	Biorad	7863-2004
Somatostatin (SOM)	polyclonal	rabbit	1:1000	Thermo Scientific	PA1-18006
Somatostatin (SOM)	monoclonal	rat	1:200	Serotec	8330-0009
Substance P (SP)	monoclonal	rat	1:200	Biorad	8450-0505
Vasoactive Intestinal Peptide (VIP)	polyclonal	mouse	1:500	Biogenesis	9535-0504
Vesicular Acetylcholine Transporter (VAChT)	polyclonal	rabbit	1:5000	Sigma	V5387
Secondary reagents					
Antigen	Fluorophore	Host	Dilution	Company	Catalog no
Mouse IgG	Alexa 488	goat	1:1000	Invitrogen	A-11001
Rat IgG	Alexa 488	goat	1:1000	Invitrogen	A-11006
Rabbit IgG	Alexa 555	goat	1:1000	Invitrogen	A-21428

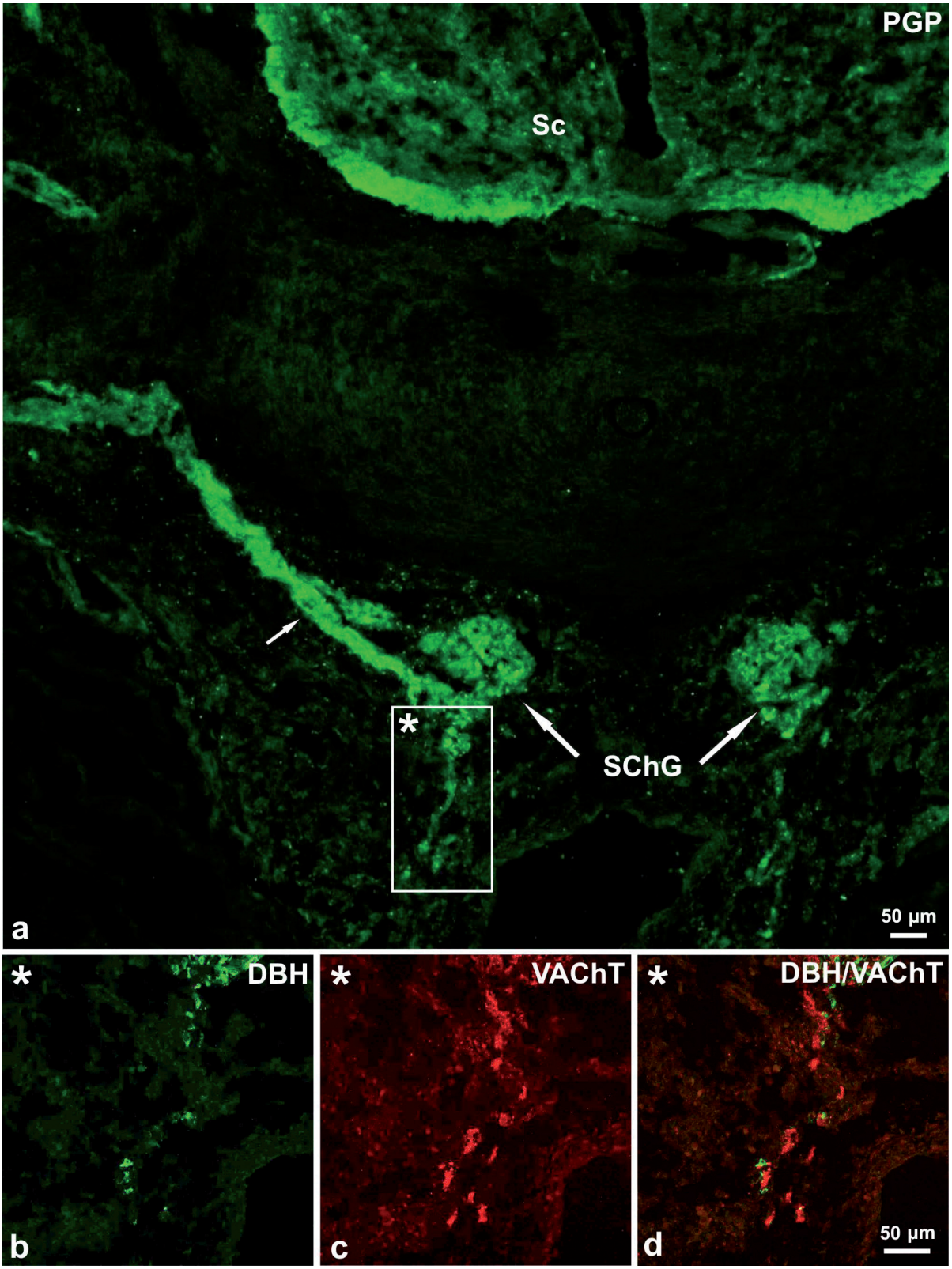

Fig. 1. Cross-section of the body cavity in a 5-week-old pig foetus. **a.** PGP-positive bundles of nerve fibres with nerve cells run ventrally from the spinal cord, towards the sympathetic chain ganglia to the abdominal cavity. The enlarged fragment **(b-d)** of the previous photo (a) shows migrating neurons and single fibres immunoreactive to dopamine-β-hydroxylase (DβH; **b**) or vesicular acetylocholine transporter (VAChT; **c**). Merged images b and c **(d)**. Sc: spinal cord; SChG: spinal chain ganglia.

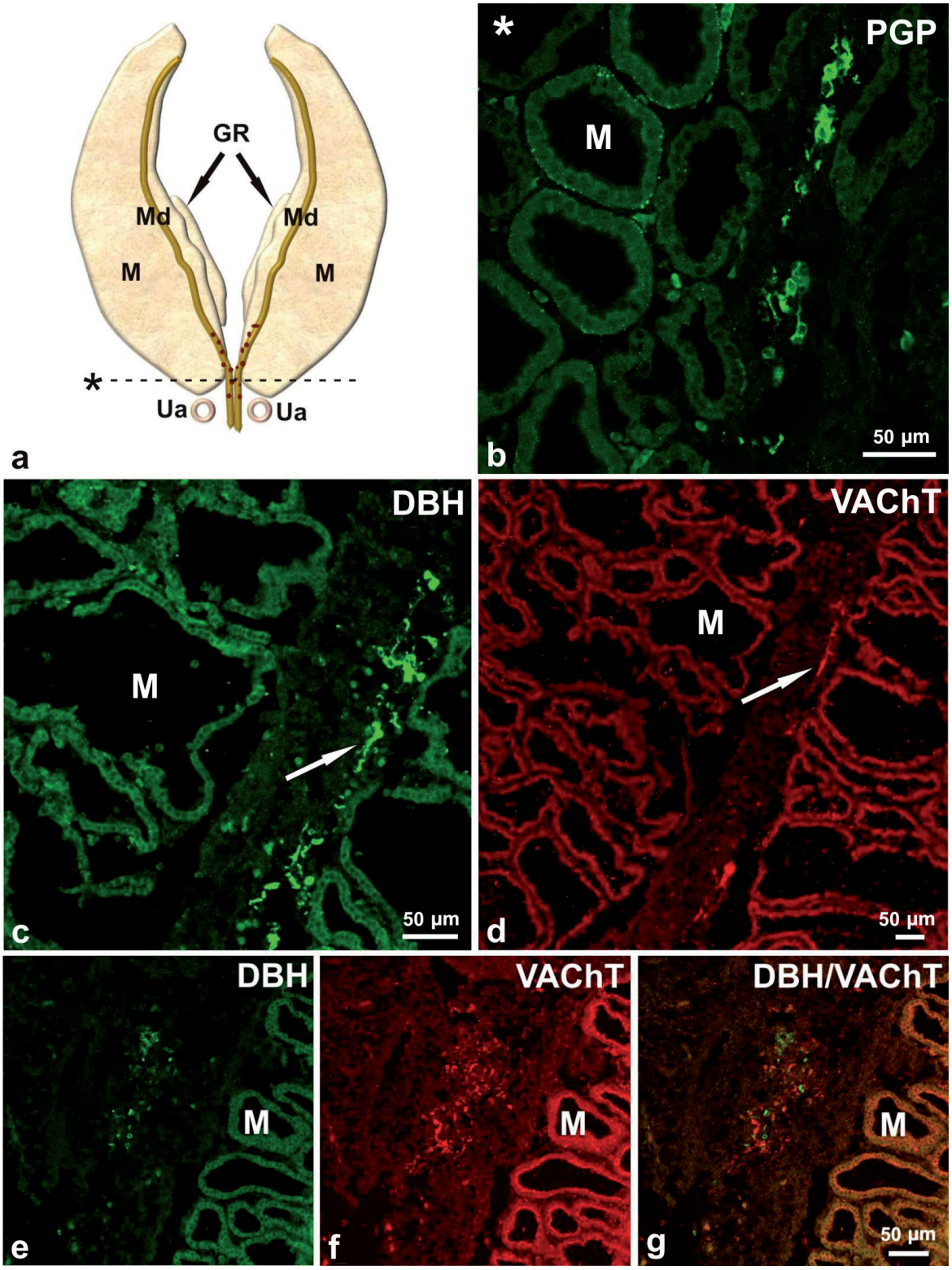

Fig. 2. Schematically illustrated ventral view of the mesonephroi with genital ridges and clustering nerve cells in the caudal part of mesonephric ducts in a 5-week-old pig foetus **(a)**. Single PGP-positive nerve cells and fibres were visible along the mesonephric ducts (b, longitudinal section). Dashed line with asterisk in schematic illustrate **(a)** show the level from which the section was used for the PGP staining **(b)**. Consecutive, longitudinal section of the mesonephroi and caudal part of mesonephric ducts immunolabelled for DβH **(c)** and VAChT **(d)**. DβH -positive neurons were more often noted than VAChT-positive. Delicate VAChT-positive nerve fibres were visible. DβH and VAChT (arrow) not co-localised in nerve structures in this stage of development **(e-g)**. M: mesonenephros, GR: genital ridges, Md: mesonephric duct, Ua: umbilical artery.

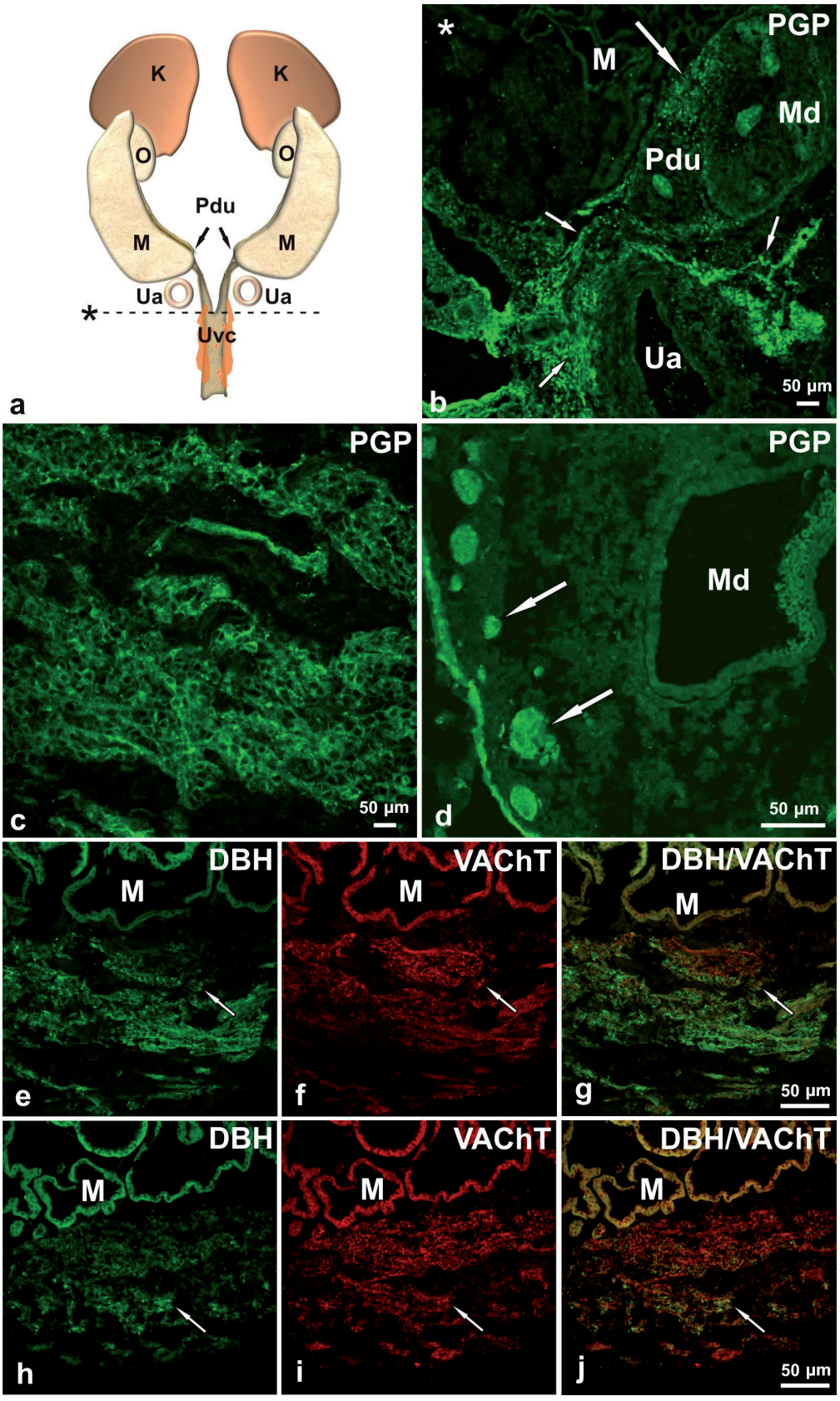

Fig. 3. Schematically illustrated **(a)** ventral view of compact group of neurons located on both sides, externally from the uterovaginal canal and caudal part of the uterine segment of the paramesonephric duct in a 7-week-old pig foetus. The illustration **(a)** also shows the developing organs of the urogenital tract for better visualization of the area of current research (kidneys, ovary and mesonephroi with uterine segment of paramesonephric ducts, followed by the uterine segment of paramesonephric ducts fused into the uterovaginal canal, a). The dashed line with an asterisk shows the level from which the cross-section was used for the PGP staining **(b)**. PGP-positive nerve structures are visible in the uterine segment of the paramesonephric duct height (long arrow) and other PGP-positive structures medially surrounding the umbilical artery (**b**, short arrows). The longitudinal section **(c)** shows a lateral view of a ganglion-like structure. Moreover, PGP-positive nerve bundles with single nerve cell bodies (arrows) were visible at the edge of the uterovaginal canal mesenchyme (**d**, cross-section). The longitudinal section of nerve structure conglomerate immunolabelled for DβH (**e**- cranial part of ganglion, h-caudal part of ganglion), VAChT (**f**-cranial part of ganglion, i-caudal part of ganglion) and merged images are visible (**g, j**, respectively). DBH-positive neurons were observed in the whole ganglion area but the vast majority of these neurons were visible in the cranial part of the ganglion **(e-g)**. VAChT-positive neurons were grouped in clusters and were mainly visible in the dorso-caudal part of the ganglion **(h-j)**. Some neurons were DβH/VAChT-positive (**e-j**, arrows). Many VAChT-positive nerve fibres were observed in the caudal but less in the middle part of the ganglion **(i)** These fibres mainly surrounded VAChT-positive, DβH/VAChT-negative and some DβH-positive neurons **(e-j)**. K: kidney, O: ovary, M: mesonephros, Pdu: uterine segment of paramesonephric duct, Ua: umbilical artery.

(Fig. 2c-g). Near (or sometimes around) the neurons, delicate, mainly VAChT-positive nerve fibres were visible (Fig. 2c-g). Other studied substances, such as NPY, SOM, GAL, VIP, NOS, CGRP, SP were not observed in neurons at this stage of prenatal development.

Seven-week-old foetuses

In 7-week-old foetuses, compact group of PGP-positive neurons were visible (Figs. 3a-c, 4; Table 2). This ganglion-like structure was observed on both sides, externally from uterovaginal canal and at the beginning of uterine segment of paramesonephric ducts (Fig. 3a). These beginning fragments of uterine segments are not yet fused part of uterovaginal canal at this stage of prenatal development (Fig. 3a). The number of neurons located in the developing PCG was 3144±213. Moreover, on the cross-section of the forming genital tract, small PGP-positive neuron clusters were visible at the edge of the uterovaginal canal mesenchyme (Fig. 3d). They contained from 3-4 to 20 neurons and were arranged mainly ventro-laterally but some of the clusters were observed on the dorso-lateral side of the mesenchyme (Fig. 3d). The neurons located in the forming PCG were mainly oval with a large nucleus. The size of these nerve cells was 7-11 μm but most of them were 8-10 μm. The neurons which were visible at the edge of the uterovaginal canal mesenchyme were slightly smaller (7-9 μm). Double immunohistochemical staining revealed that the PGP-positive neurons contained DβH (36.40±1.63%) or VAChT (17.31±1.13%) (Figs. 4, 6). Other studied biologically active substances (NPY, SOM, GAL, VIP, NOS, CGRP, SP) were not observed at this stage of development. DBH-positive neurons were observed in the whole forming ganglion area and they were grouped into larger or smaller clusters (Fig. 3e,h). VAChT-positive neurons (Fig. 3f,i) were grouped in clusters and were mainly visible in the dorso-caudal part of the ganglion (Fig. 3i).

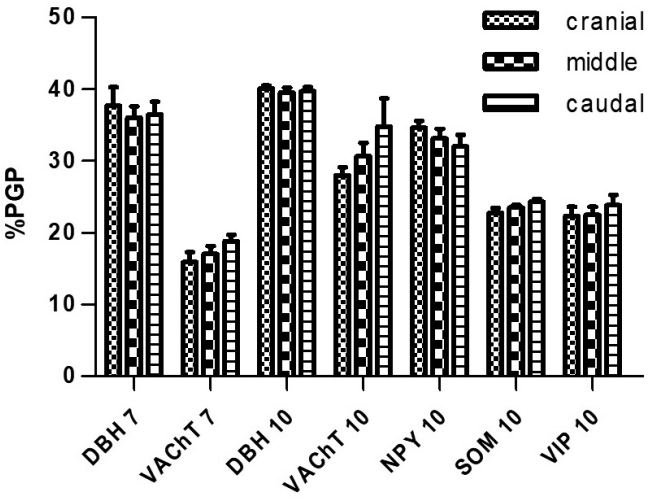

Fig. 4. Graph illustrating the data from Table 2 for the second and third prenatal development stages studied. Percentage of neurons containing the substances studied in the population of PGP-positive neurons in cranial, middle and caudal part of PCG in 7-week-old (PGP/DβH 7; PGP/VAChT 7) and 10-week-old porcine fetuses (PGP/DβH 10; PGP/VAChT 10; PGP/NPY10; PGP/SOM 10; PGP/VIP 10), p>0,05.

Table 2. Percentage of neurons containing the substances studied in the population of PGP-positive neurons in 5-, 7- (DβH; VAChT) and 10-week-old (DβH; VAChT; NPY; SOM; VIP) porcine fetuses PCG.

Stage of prenatal development		five-week-old	seven-week-old		ten-week-old	
Total number of neurons in PCG		PCG was not yet visible	3144±213		4121±259	
PGP/DβH	cranial	single neurons were visible along the caudal part of mesonephric ducts	36,40±1,63	37,18±2,55	40,26±0,73	42,54±3,09
	middle			36,03±1,62		39,05±0,64
	caudal			36,00±1,78		39,20±0,55
PGP/VAChT	cranial	single neurons were visible along the caudal part of mesonephric ducts	17,31±1,13	15,90±1,37	30,73±1,34	27,69±1,12
	middle			17,15±1,11		30,09±1,81
	caudal			18,89±0,85		34,42±3,92
DβH/VAChT	cranial	_	single neurons		few neurons	
	middle					
	caudal					
PGP/NPY	cranial	_	_		33,24±1,27	34,57±0,99
	middle					33,13±1,35
	caudal					32,01±1,65
PGP/SOM	cranial	_	_		23,6±0,44	22,88±0,66
	middle					23,59±0,35
	caudal					24,31±0,37
PGP/VIP	cranial	_	_		22,9±1,13	22,32±1,12
	middle					22,87±1,11
	caudal					23,80±1,45

Numbers displayed as mean ± SEM. Analysis of the differentiation of results between the cranial, middle and caudal part of the PCG (Student's t test; Fisher's test) showed no significant differences (p>0,05) between the average results obtained from each part of the PCG.

In the cranial or the middle part of the ganglion, far fewer VAChT-positive neurons were observed (Fig. 3f). Single DβH/VAChT-positive neurons were visible (Fig. 3e-j).

Immunohistochemical staining for PGP showed that many nerve fibres were observed throughout the forming PCG (Fig. 3c). Fewer PGP-positive fibres contained DβH and they mainly surrounded DβH-positive nerve cells or were in bundles inside the ganglion (Fig. 3e-j). The richest network of PGP-positive nerve fibres was observed in the caudal and less in the middle part of the ganglion and most of them contained immunoreactivity to VAChT (Fig. 3h-j). These fibres mainly surrounded VAChT-positive, DβH/VAChT-negative and some DβH-positive neurons. Other fibres ran in bundles through the ganglion. In the cranial part of the forming ganglion there were few VAChT-positive nerve fibres (Fig. 3e-g).

Ten-week-old foetuses

At this developmental stage, the compact group of neurons became less homogeneous (Figs. 4, 5; Table 2). It was divided into several larger and many small clusters of nerve body cells and this neural structure was more expanded along the whole uterovaginal canal and reached the initial part of the uterine canal of the paramesonephric duct (Fig. 5). The developing PCG was located externally and laterally to the mesenchyme of the paramesonephric duct and some of the externally located neuronal clusters merged with the mesenchyme. The number of neurons located in forming ganglion was about 4121±259. Some smaller clusters of neurons (15-30 neurons) were visible on the dorsal and ventral side of the mesenchyme. The size of neurons ranged from 9 to 17 μm but most of them were 11-15 μm in size. The neurons which were visible at the edge of the uterovaginal canal mesenchyme were smaller (7-9 μm).

Double immunohistochemical staining revealed that the PGP-positive neurons located in the forming PCG contained DβH (40.26±0,73%) and VAChT (30.73±1.34%) (Figs. 4, 6). In addition to basic biologically active substances, it was observed that neurons were also immunoreactive for NPY, VIP and SOM at this stage of development (Figs. 4, 7, 8). DβH-positive neurons (Fig. 8a,d,j) were dispersed irregularly in the ganglion and usually formed groups of up to several dozen cells. The most DβH-positive neurons were observed in the cranial part of the ganglion. Low-intensity DBH-positive cells were also observed at this stage of development (Fig. 8a). Small clusters of DβH-positive neurons were visible in the paramesonephric duct mesenchyme. VAChT-positive neurons (Fig. 8b,h,n) were mainly visible in the caudal part of the ganglion and the number of VAChT-positive neurons decreased cranially. These neurons formed the large clusters which were visible on the side of the ganglion, away from the edge of the paramesonephric duct mesenchyme (Fig. 8b). Single VAChT-positive neurons were observed on the edge of the mesenchyme. Some neurons were DβH/VAChT-positive and these neurons were low-intensity to DBH (Fig. 8a-c). The irregular network of numerous PGP-positive nerve fibres was observed throughout the ganglion. The majority of them were located in the caudal and less in the middle part of the ganglion and most of them contained immunoreactivity to VAChT. VAChT-positive nerve fibres formed a rich network which mainly surrounded VAChT-positive and DβH-negative neurons (Fig. 8a-c) but these nerves were also observed in the parts of the ganglion where DβH-positive neurons occur. In the cranial part of the ganglion there were few VAChT-positive nerve fibres. Fewer PGP-positive fibres contained DβH, and they mainly surrounded DβH-positive nerve cells or were in bundles

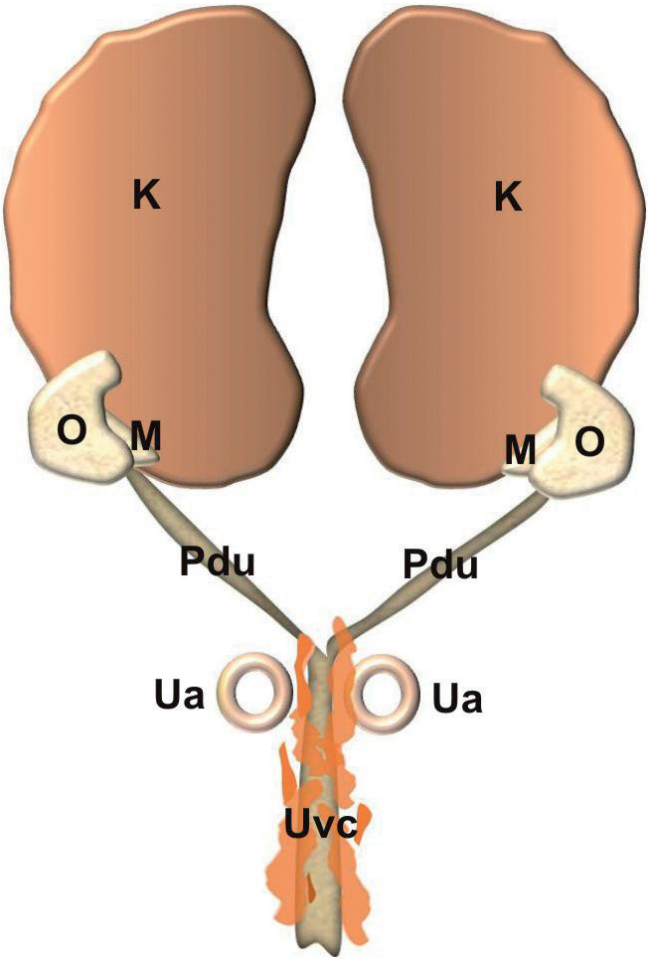

Fig. 5. Schematically illustrated ventral view of developing paracervical ganglion (PCG) located on both sides, externally from the uterovaginal canal and caudal part of the uterine segment of the paramesonephric duct in a 10-week-old pig foetus. The illustration also shows the developing organs of the urogenital tract for better visualization of the area of current research (kidneys, ovary, uterine segment of paramesonephric ducts, followed by the uterine segment of paramesonephric ducts fused into the uterovaginal canal). K: kidney, O: ovary, M: mesonephros, Pdu: uterine segment of paramesonephric duct, Ua: umbilical artery, Uvc: uterovaginal canal.

inside the ganglion.

NPY-positive neurons (33.24±1,27%) (Figs. 4, 7, 8e), are the most frequently observed group of neurons compared to SOM- or VIP-positive neurons in 10-week-old foetuses. NPY-positive neurons simultaneously contained DβH (Fig. 8d-f). They were most often seen on the periphery of the ganglion. Single NPY-positive neurons were VAChT- (Fig. 8e,h) and VIP-positive in this stage of development. Many NPY-positive fibres were visible throughout the ganglion. Few NPY-positive fibres were observed in the uterovaginal canal mesenchyme of the paramesonephric duct. They were usually positive to DβH.

SOM-positive neurons (23.6±0,44%) (Figs. 4, 7, 8k) were observed in the outer parts of the ganglion and formed clusters. These neurons also contained VAChT (Fig. 8h,k), less DβH (Fig. 8j-l) and single VIP. Single SOM-positive neurons were negative to DβH or VAChT. No presence of NPY was noted in SOM-positive neurons. Generally, the SOM-positive nerve fibres surrounded SOM-positive neurons and co-localised with VAChT. Single SOM-positive nerve fibres were visible in surrounding zones of SOM-positive neurons.

VIP presence was found in about 22.9±1,13% (Figs. 7, 8m) of all neurons in the forming PCG. These neurons were mainly visible in ganglion areas where VAChT-positive neurons were observed. The majority of VIP-positive nerve body cells were cholinergic (Fig. 8m-o). VIP-positive neurons were weakly immunoreactive. Single VIP-positive neurons colocalised with NPY, SOM or DβH. A few VIP-positive nerve fibres mainly surrounded VIP/VAChT- or VAChT-positive neurons and colocalised with VAChT (Fig. 8m-o). Many nerve fibres containing VIP and VAChT were observed in the mesenchyme of the uterovaginal canal of paramesonephric ducts.

No GAL, NOS, CGRP or SP were observed in PCG neurons at this stage of development.

Discussion

As mentioned earlier, in the juvenile pig, it was found that the pelvic neurons additionally form numerous scattered ganglia in the pelvic cavity (Majewski, 1997; Wasowicz et al., 1998, 2002; Podlasz and Wąsowicz, 2008) and detailed studies in this species have shown that at the level of the uterovaginal junction in the parametrium, neurons group into large clusters on both sides of the organ and form a PCG (Łakomy and Szatkowska, 1992; Majewski, 1997; Podlasz and Wąsowicz, 2008; Wąsowicz et al., 2002). In the current study, the view of the pelvic plexus with PCG in porcine female foetuses in the studied developmental stages appear quite different. In the 5-week-old foetus, besides a few PGP-positive neurons which contained DBH or VAChT, no other neuronal structures were observed in the external part of the mesenchyme surrounding the mesonephric ducts. However, it is visible that at this stage of development neurons migrate ventrally from SChG towards the body cavity, but the target destination is difficult to predict. A similar view of forming neuronal structures was visible in mouse in 10.5 dpc (Itäranta et al., 2009; Wiese et al., 2017). In the 7-week-old porcine foetus, the nervous structure is visible at the level of the

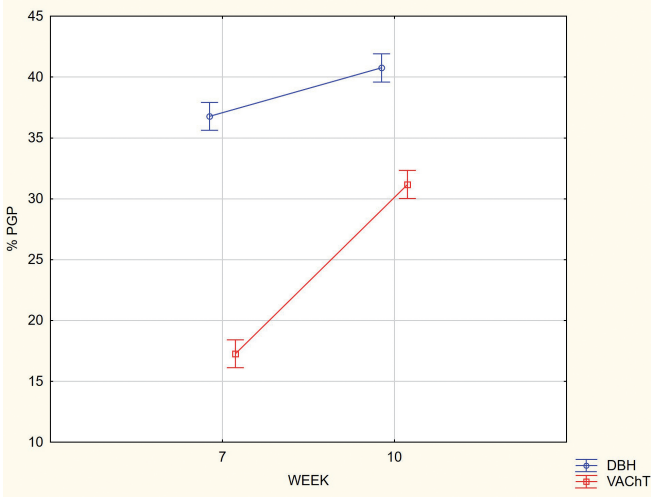

Fig. 6. The number of PGP/DβH- or PGP/VAChT-positive neurons in PCG of 7- and 10-week-old foetuses. This study showed a significant increase in the number of cholinergic neurons between week 7 and week 10 of prenatal development as opposed to DβH-positive neurons, whose number increased only slightly. A two-factor variance analysis (Fisher's test) was applied. The correlation between both factors (time, substance) was found to be statistically significant at $p<0.05$.

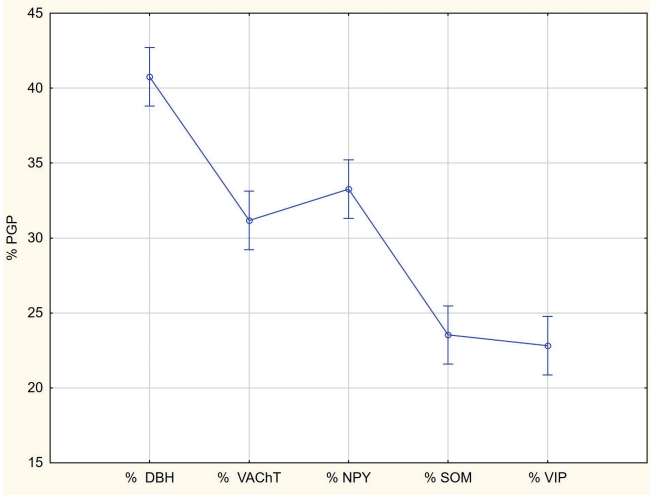

Fig. 7. The analysis of diversification of the biologically active substances present in PGP-positive neurons of the PCG in 10-week-old foetuses (one-factor variance analysis; Fisher's test) showed a significant differentiation of mean results ($p<0.05$). Moreover, three homogeneous groups of means were identified (Bonferroni's test): DβH; VAChT and NPY; SOM and VIP. It may confirm the observations that one neuron may contain two or more various substances.

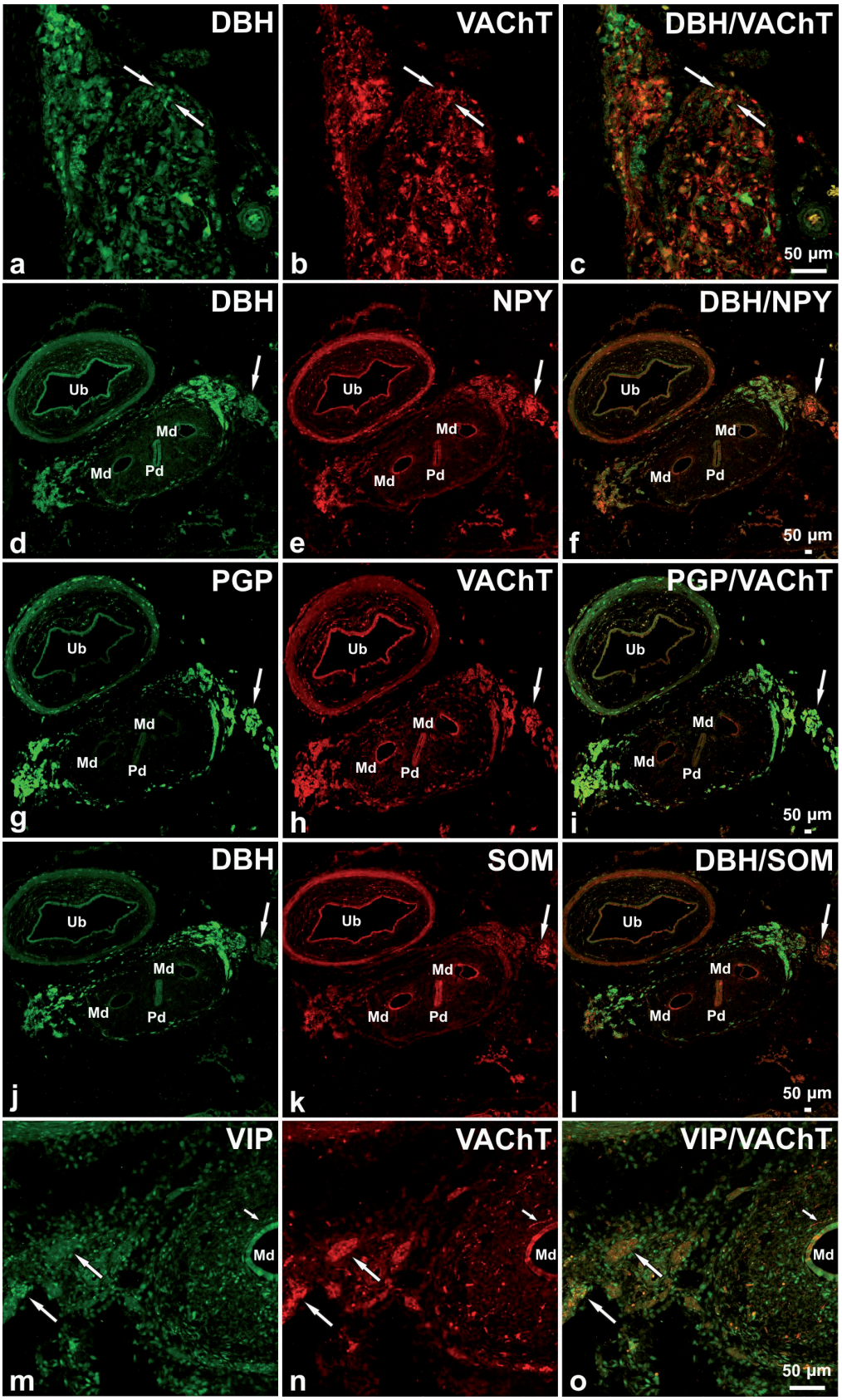

Fig. 8. A cross-section of the uterovaginal canal and PCG in a 10-week-old pig foetus. DβH- **(a)** and/or VAChT-positive **(b)** nerve structures in PCG. The arrows show DβH/VAChT-positive neurons in PCG **(a-c)**. NPY-positive neurons simultaneously contained DβH **(d-f)**. They were most often seen on the periphery of the ganglion. Single NPY-positive neurons **(e)** were VAChT-positive (h, consecutive section). Many NPY-positive fibres were visible throughout the ganglion **(e)**. A few NPY-positive fibres were observed in the uterovaginal canal mesenchyme of the paramesonephric duct. They were usually positive to DβH **(d)**. SOM-positive neurons were observed in the outer parts of the ganglion and formed groups **(k)**. These neurons often contained VAChT (h, consecutive section) and less DβH **(j)**. VIP-positive neurons were weakly immunoreactive and were mainly visible in ganglion areas where VAChT-positive neurons were observed (**m-o**, long arrows). A few VAChT/VIP-positive nerve fibres were visible in uterovaginal canal mesenchyme (**m-o**, short arrow) Merged images: a and b **(c)**; d and e **(f)**; g and h **(i)**; j and k **(l)**; m and n **(o)**.

uterovaginal canal and not yet fully fused beginning part of the uterine segment of the paramesonephric ducts. This bilateral nervous structure (compact group of neurons) is uniform and adheres to the mesenchyme of paramesonephric ducts. This observation strongly suggests that the PCG and pelvic plexus are forming at this stage of development. Previous studies dealing with the development of internal female genital organs in porcine foetuses (Franke-Radowiecka et al., 2019) revealed that at this stage of development some PGP-positive nerves penetrated the mesenchyme of paramesonephric ducts along their entire length. The nerve fibres, which were observed in mesenchyme of the uterovaginal canal (with high probability) are axons of nerve body cells derived from developing PCG and mainly contained VAChT. Comparing the prenatal development of human, mouse and pig, it seems that the pelvic plexus starts to develop between 1/3 to half of the prenatal period. In male human foetuses nerve cells in the body cavity in the vicinity of the developing prostate were visible in the 13th week of foetal life (Jen and Dixon, 1995) and a week later some neuronal clusters were observed in the mesenchyme of the uterovaginal canal of the paramesonephric ducts in female foetuses (Olfat and Rahman, 1978). At this developmental period in the human foetus only DβH and VAChT were found in neurons and nerve fibres of this region (Olfat and Rahman, 1978). In mice, between 11.5 and 13dpc, NCSCc have passed to the hindgut and coalesce to form the pelvic plexus primordium between the hindgut and urogenital sinus (Anderson et al., 2006; Wang et al., 2011; Wiese et al., 2012, 2017) then some neurons and nerve fibres enter the urogenital sinus mesenchyme (Itäranta et al., 2009; Wiese et al., 2017).

In 10-week-old porcine foetuses, further changes in the formation of PCG were observed. PCG became less uniform and stretched and began dividing into smaller clusters of nerve cells. This neural structure was more expanded along the whole uterovaginal canal and slightly reached up to the caudal part of the uterine segment of the paramesonephric duct. At this time also, as we know from previous studies (Franke-Radowiecka et al., 2019) the most PGP-positive nerve fibres were observed at the uterovaginal canal height and fewer at the uterine and tubal segments of paramesonephric ducts. Many PGP-positive nerve fibres penetrated the mesenchyme and were regularly distributed there (Franke-Radowiecka et al., 2019). A new aspect in developing PCG is the appearance of other biologically-active substances in neurons and nerve fibres in the third studied period, which correlates with other foetal studies and emerging neurotransmitters, most often in the second half of prenatal development (Jen and Dixon, 1995; Keast et al., 2015), but this aspect will be discussed later.

The number of pelvic plexus neurons increases during prenatal development, which was confirmed by earlier rodent studies (Keast, 2009) and it continues to increase in postnatal life (Keast, 1999, 2009; Wiese et al., 2017; Yan and Keast, 2008). In the present research, the number of PCG neurons, as a part of the pelvic plexus, also changed from about 3144 in 7-week-old foetuses to 4121 in 10-week-old foetuses and, presumably, this number will at least double, as noted in mice (Yan and Keast, 2008). In piglets, the authors (Podlasz and Wąsowicz, 2008) were not able to count all PCG neurons due to their dispersion and difficulty in identifying whether selected groups of neurons belong to PCG or they composed smaller clusters of the pelvic plexus. Due to this fact, despite the nerve cells being counted especially in the third studied period, where the forming PCG began dividing into smaller clusters of nerve cells, it is difficult to assess whether all of the counted neurons belong to PCG or if some of them (lying on the periphery) will constitute separate nerve structures of the pelvic plexus. However, counting neurons allowed confirmation whether the number of nerve cells was modified. It is known that during prenatal life, the pelvic plexus undergoes reorganization, i.e. some nerve cells disappear due to the process of apoptosis and new ones appear in their place (Shakhova and Sommer 2010; Wiese et al., 2012, 2017). This phenomenon is related to the intensive development of pelvic ganglia during this period where neuronal differentiation is an ongoing process concurrent with sacral NCPCs migration, rather than a stepwise series of events that occur after sacral NCPCs coalesce to form pelvic ganglia (Wiese et al., 2017). This fact can also explain the extent of neuron size at a given stage, i.e. 7-9 μm in the first studied period, 8-10 μm in the second period and 11-15 μm in the third period.

In the immature female pig, PCG contains approximately 23% adrenergic and 77% cholinergic neurons (Podlasz and Wasowicz, 2008). Depending on the species, there is a slightly different percentage (Papka et al., 1985, 1987; Wanigasekara et al., 2003; Elfvin et al., 1997). It was also found that most of the adrenergic neurons were located in the cranial part of the porcine PCG and their number gradually decreased towards the caudal direction. In contrast, the cholinergic nerve cells were more abundant in the caudal part of the ganglion (Wasowicz et al., 1998, 2002; Podlasz and Wasowicz, 2008). This distribution pattern can be ascertained already in the 7th week of prenatal development, where a slight dominance of VAChT-positive neurons in the caudal part of the ganglion was observed. In the 10-week-old foetuses, the presence of DβH-positive neurons in the cranial part and VAChT-positive neurons in the caudal part of PCG was more numerous. The existence of these two regions in the ganglion, the adrenergic and cholinergic one, is probably related to the origin and pathways of the preganglionic fibres. The sympathetic preganglionic fibres, supplying mostly the adrenergic neurons, run predominantly via the more cranially located hypogastric nerve, while the parasympathetic preganglionic axons travel via the more caudally located pelvic nerve (Keast, 1995; Podlasz and Wasowicz, 2008).

In porcine foetuses, 36.40% DβH- and 17.31% VAChT-positive and 40.26% DβH- and 30,73% VAChT-positive nerve cell bodies were observed in 7-week-old and 10-week-old foetuses, respectively. It is known that in porcine PCG there are no non-adrenergic and non-cholinergic neurons (Podlasz and Wasowicz, 2008). The situation in the foetuses PCG could be a consequence of intensive changing, neuronal differentiation, migration and maturation of neurons (Wiese at al., 2017). Taking into account the percentage of substances, perhaps some of the neurons of the forming ganglion are still neurochemically undetermined, hence the higher percentage of adrenergic neurons in the foetus relative to the juvenile pig and the ever-increasing number of cholinergic neurons. In addition, this study also revealed a significant increase in the number of cholinergic neurons between week 7 and 10 of prenatal development, in contrast to DβH-positive neurons, the number of which increased slightly. Moreover, DβH-positive neurons were evenly distributed throughout the ganglion of the 7-week-old foetuses, and low-intensity DβH-positive neurons were observed in the 10-week-old foetuses. These observations may also indicate a progressive change in the neurotransmitter phenotype.

The final phenotype of sympathetic or parasympathetic neurons depends on signals derived from the target tissue (Anderson et al., 2002; Luther and Birren, 2009; Young et al., 2011) and these retrograde signals comprise a range of growth factors and cytokines (Young et al., 2011). One of the best-known examples of the influence of a target tissue on the neurochemical coding of neurons are the nerve cells supplying sweat glands or the periosteum in new-born rodents, where adrenergic neurons were found to up-regulate cholinergic synthesizing enzymes and transporters, and consequently become cholinergic (Francis and Landis, 1999). This data may explain the presence of DβH/VAChT-positive neurons in the studied developmental stages which presumably undergo transformation of the neurotransmitter phenotype. Another example is the ciliary ganglion in the chick where the network of transcription factors (Ascl1, Phox2a, Phox2b) initially control the neuronal differentiation, which is similar to factors that initially control the differentiation of noradrenergic sympathetic neurons, although the mature ciliary ganglion neurons are cholinergic in nature (Howard, 2005; Young et al., 2011). Regarding pelvic ganglia, it is only known that the sympathetic neurons in late embryonic and neonatal mice or mature rats show an axon outgrowth response to NGF *in vitro* whereas, the pelvic parasympathetic neurons outgrowth response to neurturin but not to NGF (Meusburger and Keast, 2001; Steward et al., 2008; Yan and Keast, 2008; Young et al., 2011). Nonetheless, the mechanisms regulating the neurotransmitter phenotype of sympathetic and parasympathetic pelvic neurons have not yet been identified (Yan and Keast, 2008; Young et al., 2011).

In 10-week-old foetuses, besides classical neurotransmitters, PCG neurons contained NPY (33.24%), SOM (23.6%) and VIP (22.9%). In the PCG of juvenile pigs, 75% of neurons contained NPY, 67% - SOM and all cholinergic neurons were VIP-positive (about 77%) (Podlasz and Wasowicz, 2008). In the foetal PCG, NPY was abundant in both adrenergic and cholinergic neurons. SOM was present mainly in cholinergic neurons and VIP was determined only in cholinergic nerve cells (Podlasz and Wasowicz, 2008). In the third stage of prenatal development studied, observations on consecutive sections revealed the presence of DβH/VIP-, DβH/SOM- or only SOM-positive neurons, which were not observed in the PCG of juvenile pigs (Podlasz and Wasowicz, 2008). It is clearly evident that the foetal PCG neurons are just starting to define their neurochemical phenotype.

GAL, NOS, CGRP and SP were not observed in PCG in any period studied. In PCG of juvenile pigs, GAL occurs only in small, adrenergic neurons, possibly interneurons. GAL inhibits noradrenaline release by hyperpolarisation of the neuronal cell membrane and can then moderate the function of adrenergic neurons (Reimann and Schneider, 1993). Twenty five percent of juvenile pig PCG neurons contained nNOS and all were cholinergic in nature (Podlasz and Wasowicz, 2008). In the female reproductive tract, for instance, nitric oxide affects the relaxation of the uterine muscles (Wasowicz et al., 2002). Considering the processes taking place in PCG in week 10 of prenatal development (proliferation and maturation of neurons) as well as the fact that the urogenital organs begin, at this time, to undergo intensive development, the presence of GAL or NOS in the neurons is a rather unexpected phenomenon. SP and CGRP nerve fibres were abundant and were distributed mainly around the adrenergic neurons. They are probably sensory fibres, and it is known, from previous studies dealing with the innervation of the urinary bladder in human foetuses (Keast et al. 2015), heart (Franke-Radowiecka et al., 2020) and the reproductive system in porcine foetuses (Franke-Radowiecka et al., 2019) that autonomic nervous structures develop much earlier than the sensory innervation.

Current research has also shown that few DβH/NPY- and many VAChT/VIP-positive nerve fibres penetrate the mesenchyme of the uterovaginal canal. In general, such neurochemically coded nerve fibres play presumably a vasomotor function (Wasowicz et al., 2002), but no relevant data pertaining to foetuses are available. Presumably, these fibres are just axons of neurochemically determined nerve cell bodies (DβH/NPY- and VAChT/VIP-positive) which have reached their target tissues and may give the next phase of the reproductive system organs development. In 10-week-old porcine foetuses (starting at the last 1/3 of the prenatal period) b dynamic innervation development of each segment of paramesonephric ducts begins (Franke-Radowiecka et al., 2019) and visible changes in the number and coding of PCG neurons were observed. Furthermore, this is a period when dynamic changes

occur in the development of female internal genital organs. For example, a previous study dealing with the uterine epithelium in the domestic cat during prenatal development (Prozorowska et al., 2019) showed that the differentiation of this epithelium into the mucosal epithelium starting after 42 dpc (second half of prenatal development) and lasting until the end of the prenatal period (Prozorowska et al., 2019). Additionally, several reports (Jen and Dixon, 1995; Arrighi et al., 2008) have noted that some neuropeptides appear in the nerve structures of the genitourinary tract just in the second half of pregnancy, such as NPY, SOM or VIP and others, including GAL, NOS, CGRP or SP appear in the perinatal period or later, but it is still unknown what the role play biological active substances appearing at a specific time in these nerve structures.

The mechanisms and factors responsible for the projection of sympathetic axons to their targets are well understood. Artemin (Yan et al., 2003), Neurotrophin-3 (Kuruvilla et al., 2004) or Endothelin-3 (Makita et al., 2008) are factors associated with blood vessels inducing axon outgrowth. Another group of factors, such as nerve growth factor (NGF) or Bax, may then be responsible for the entry of sympathetic axons into the specific target tissue (Young et al., 2011). Less is known about the mechanisms and factors responsible for the projection of parasympathetic axons to their targets in mammals (Hashino et al., 2001; Young et al., 2011) but it is known that glial cell line-derived neurotrophic factor (GDNF) appears to act as a chemoattractant to promote the growth of axons towards their targets (Hashino et al., 2001; Young et al., 2011) and neurturin appears to be required for the maintenance, axon growth and branching of some parasympathetic ganglia (Yan and Keast, 2008). The absence of any factor interferes with the migration, proliferation and projection of the axons to their targets. For instance, inactivation of the genes encoding Artemin leads to partial disruption of axon projection along blood vessels (Honma et al., 2002), lack of NT-3 causes a partial disruption of sympathetic axon projection to their target, while a lack of neurturin leads to a reduced number of parasympathetic neurons (Lahtennmaki et al., 2007; Young et al., 2011). However little is known about the factors and mechanisms regulating the formation and development of pelvic ganglia, such as the porcine PCG. In the light of the existing knowledge it can be assumed that the lack of some factors may cause developmental abnormalities and may have a negative impact on subsequent innervation of the urogenital organs, which can finally cause disturbances in the urogenital system development. It should be mentioned that there are many Müllerian duct (paramesonephric ducts) anomalies, such as uterine cavity abnormalities, uterine and vaginal agenesis or duplication (Chmel et al., 2019). Most disorders of the paramesonephric ducts are genetic, but we do not know if, in some cases, it is associated with the abnormally developing nervous system, particularly PCG, which is strongly involved in the innervation of the uterus. The reproductive process is an important element in animal husbandry. A well-formed and functioning reproductive system is a guarantee of having healthy offspring. A detailed knowledge on the morphology of PCG in the porcine foetus, and the migration factors and mechanisms regulating the phenotype of neurotransmitters in this ganglion would help to better understand, for instance, processes important for regenerative nerve structure therapies, such as those dealing with the formation of nerve structures, and the possibilities of their renewal and reconstruction.

In summary, for the first time, the morphology of PCG formation in the porcine foetus has been described in three stages of development. Dynamic changes in the number of neurons and their sizes were also noted, as well as the changes in immunochistochemical coding of maturing neurons. These studies bring new data to the scarce knowledge dealing with the development of genitourinary organ innervation, especially in pigs.

Acknowledgements. The authors would like to thank Anna Przyborowska, Natalia Kasica-Jarosz and Aleksander Penkowski for their contributions in preparing this paper.

This publication was supported by RID (Project financially co-supported by Minister of Science and Higher Education in the range of the program entitled "Regional Initiative of Excellence" for the years 2019-2022). Project No. 010/RID/2018/19, amount of funding 12.000.000 PLN.

Conflict of interests. The authors have no conflict of interest to declare.

References

Anderson C., Penkethman S., Bergner A., McAllen R. and Murphy S. (2002). Control of postganglionic neurone phenotype by the rat pineal gland. Neuroscience 109, 329-337.

Anderson R., Stewart A. and Young H. (2006). Phenotypes of neural-crest-derived cells in vagal and sacral pathways. Cell Tissue Res. 323, 11-25.

Arrighi S., Bosi G., Cremonesi F. and Domeneghini C. (2008). Immunohistochemical study of the pre- and postnatal innervation of the dog lower urinary tract: Morphological aspects at the basis of the consolidation of the micturition reflex. Vet. Res. Commun. 32, 291-304.

Bell C. (1972). Autonomic nervous control of reproduction: Circulatory and other factors. Pharmacol. Rev. 24, 657-736.

Botti M., Ragionieri L., Gazza F., Acone F., Minelli L. and Panu R. (2009). Striated perineal muscles: location of autonomic, sensory, and somatic neurons projecting to the male pig bulbospongiosus muscle. Anat. Rec. (Hoboken) 292, 1756-1763.

Britsch S., Goerich D., Reithmacher D., Peirano R., Rossner M., Nave, K., Birchmeier C. and Wegner M. (2001). The transcription factor Sox10 is a key regulator of peripheral glial development. Genes Dev. 15, 66-78.

Chmel R., Pastor Z., Mužík M., Brtnický T. and Nováčková M. (2019). Syndrome Mayer-Rokitansky-Küster-Hauser - uterine and vaginal agenesis: current knowledge and therapeutic options. Ceska Gynekol. 84, 386-392.

Davies A. (2009). Extracellular signals regulating sympathetic neuron

survival and target innervation during development. Auton. Neurosci. 151, 39-45.

Elfvin L., Holmberg K., Emson P., Schemann M. and Hökfelt T. (1997). Nitric oxide synthase, choline acetyltransferase, catecholamine enzymes and neuropeptides and their colocalization in the anterior pelvic ganglion, the inferior mesenteric ganglion and the hypogastric nerve of the male guinea pig. J. Chem. Neuroanat. 14, 33-49.

Evans H. and Sack W. (1973). Prenatal development of domestic and laboratory mammals: Growth curves, external features and selected references. Anat. Histol. Embryol. 2, 11-45.

Francis N. and Landis S. (1999). Cellular and molecular determinants of sympathetic neuron development. Annu. Rev. Neurosci. 22, 541-566.

Franke-Radowiecka A. (2011). Immunohistochemical characterisation of dorsal root ganglia neurons supplying the porcine mammary gland. Histol. Histopathol. 26, 1509-1517.

Franke-Radowiecka A., Giżejewski Z., Klimczuk M., Dudek A., Zalecki M., Jurczak A. and Kaleczyc J. (2016). Morphological and neuroanatomical study of the mammary gland in the immature and mature European beaver (*Castor fiber*). Tissue Cell 48, 552-557.

Franke-Radowiecka A., Prozorowska E., Zalecki M., Jackowiak H. and Kaleczyc J. (2019). Innervation of internal female genital organs in the pig during prenatal development. J. Anat. 235, 1007-1017.

Franke-Radowiecka A., Zmijewska N., Zubkiewicz T., Zalecki M., Klimczuk M., Listowska Ż. and Kaleczyc J. (2020). Nerve structures of the heart and their immunohistochemical characterization in 10-week-old porcine fetuses. C R Biol. 343, 53-62.

Hashino E., Shero M., Junghans D., Rohrer H., Milbrandt J. and Johnson Jr (2001). GDNF and neurturin are target-derived factors essential for cranial parasympathetic neuron development. Development 128, 3773-3782.

Honma Y., Araki T., Gianino S., Bruce A., Heuckeroth R., Johnson E. and Milbrandt J. (2002). Artemin is a vascular-derived neurotropic factor for developing sympathetic neurons. Neuron 35, 267-282.

Howard M. (2005). Mechanisms and perspectives on differentiation of autonomic neurons. Dev. Biol. 277, 271-286.

Itäranta P., KeijoViiria K., Kaartinenb V. and Vainio S. (2009). Lumbo-sacral neural crest derivatives fate mapped with the aid of Wnt-1 promoter integrate but are not essential to kidney development. Diferrentiation 77, 199-208.

Jen P. and Dixon J. (1995). Development of peptide-containing nerves in the human fetal prostate gland. J. Anat. 187, 169-179.

Kaleczyc J., Wąsowicz K., Klimczuk M., Czaja K. and Lakomy M. (2003) Immunohistochemical characterisation of cholinergic neurons in the anterior pelvic ganglion of the male pig. Folia Histochem. Cytobiol. 41, 65-72.

Kaleczyc J., Kasica-Jarosz N., Pidsudko Z., Dudek A., Klimczuk M. and Sienkiewicz W. (2020) Effect of castration on pelvic neurons in the male pig. Histochem. Cell Biol. 153, 135-151.

Kanerva L. (1972) Ultrastructure of sympathetic ganglion cells and granule-containing cells in the paracervical (Frankenhäuser) ganglion of the newborn rat. Z Zellforsch Mikrosk Anat. 126, 25-40.

Kanerva L. and Teravainen H. (1972). Electron microscopy of the paracervical (Frankenhäuser) ganglion of the adult rat. Z Zellforsch Mikrosk. Anat. 129, 161-177.

Kanerva L., Lietzen R. and Teravainen H. (1972). Catecholamines and cholinesterases in the paracervical (Frankenhäuser) ganglion of normal and pregnant rats. Acta Physiol. Scand 86, 271-277.

Kapur R. (2000). Colonization of the murine hindgut by sacral crest-derived neural precursors: Experimental support for an evolutionarily conserved model. Dev. Biol. 227, 146-155.

Keast J. (1995). Visualization and immunohistochemical characterization of sympathetic and parasympathetic neurons in the male rat major pelvic ganglion. Neuroscience 66, 655-662.

Keast J. (1999) Unusual autonomic ganglia: connections, chemistry, and plasticity of pelvic ganglia. Int. Rev. Cytol. 193, 1-69.

Keast J. (2009). Neurotrophic factor mechanisms underlying the development and plasticity of pelvic ganglia. Luts 1, 48-49.

Keast J., Smith-Anttila C. and Osborne P. (2015). Developing a functional urinary bladder: a neuronal context. Front. Cell Dev. Biol. 3, 53.

King P., Redden D., Palmgren J. S., Naborsa L. B. and Lennond V. (1999). Hu antigen specificites of ANNA-I autoantibodies paraneoplastic neurological disease. J. Autoimmun. 13, 435-443.

Klimczuk M., Kaleczyc J., Franke-Radowiecka A., Podlasz P. and Łakomy M. (2005). Immunohistochemical characterisation of cholinergic nerve fibres supplying accessory genital glands in the pig. Vet. Med. Czech 61, 361-373.

Kuruvilla R., Zweifel L., Glebova N., Lonze B., Valdez G, Ye H. and Ginty D. (2004). A neurotrophin signaling cascade coordinates sympathetic neuron development through differential control of TrkA trafficking and retrograde signaling. Cell 118, 243-255.

Lahteenmaki M., Kupari J. and Airaksinen M. (2007). Increased apoptosis of parasympathetic but not enteric neurons in mice lacking GFRalpha2. Dev. Biol. 305, 325-332.

Luther J. and Birren S. (2009). Neurotrophins and target interactions in the development and regulation of sympathetic neuron electrical and synaptic properties. Auton. Neurosci. 151, 46-60.

Łakomy M. and Szatkowska C. (1992). Cytoarchitecture of the paracervical ganglion (Frankenhauser) of pig. Arch. Vet. Pol. 32, 31-39.

Majewski M. (1997). Afferentne i efferentne unerwienie jajnika świni - źródła pochodzenia i kodowanie chemiczne. Praca habilitacyjna. Acta Acad. Agricult. Tech. Olst. Veterinaria 24 (Suppl. B) 1-123.

Makita T., Sucov H., Gariepy C., Yanagisawa M. and Ginty D. (2008). Endothelins are vascular-derived axonal guidance cues for developing sympathetic neurons. Nature 452, 759-763.

Meusburger S. and Keast J. (2001). Testosterone and nerve growth factor have distinct but interacting effects on structure and neurotransmitter expression of adult pelvic ganglion cells *in vitro*. Neuroscience 108, 331-340.

Mitchell B. (1993). Morphology and neurochemistry of the pelvic, and paracervical ganglia. Histol. Histopathol. 8, 761-773.

Mitchell B. and Ahmed E. (1992). An immunohistochemical study of the catecholamine synthesizing enzymes and neuropeptides in the female guinea-pig uterus and vagina. Histochem. J. 24, 361-367.

Mitchell B., Ahmed E. and Stauber V. (1993). Projections of the guinea-pig paracervical ganglion to pelvic viscera. Histochem. J. 25, 51-56.

Nouhouayi Y. and Negulesco I. (1983). Morphological and ultrastructural study of the neural pelvic plexus in the male white mouse. Z. Mikrosk. Anat. Forsch. 97, 520-528.

Olfat S. and Rahman S. (1978). Pre-natal innervation of the human female genital tract. Acta Anat. 101, 359-371.

Papka R., Cotton J. and Traurig H. (1985). Comparative distribution of neuropeptide tyrosine-, vasoactive intestinal polypeptide-, substance P-immunoreactive, acetylcholinesterase-positive and noradrenergic nerves in the reproductive tract of the female rat. Cell Tissue Res. 242, 475-490.

Papka R., Traurig H. and Klenn P. (1987). Paracervical ganglia of the

female rat: Histochemistry and immunohistochemistry of neurons, SIF cells, and nerve terminals. Am. J. Anat. 179, 3 243-257.

Pidsudko Z., Listowska Ż., Franke-Radowiecka A., Klimczuk M., Zalecki M. and Kaleczyc M. (2019). Distribution and chemical coding of urinary bladder apex-projecting neurons in aorticorenal and testicular ganglia of the male pig. Pol. J. Vet. Sci. 22, 427-430.

Podlasz P. and Wasowicz K. (2008). Neurochemical characteristics of paracervical ganglion in the pig. Veterinarni Med. 53, 135-146.

Prozorowska E., Ratajczak M. and Jackowiak H. (2019). Ultrastructural study of uterine epithelium in the domestic cat during prenatal development. J. Morphol. 130, 49-61.

Ragionieri L., Botti M., Gazza F., Sorteni C., Chiocchetti R., Clavenzani P., Bo Minelli L. and Panu R. (2013). Localization of peripheral autonomic neurons innervating the boar urinary bladder trigone and neurochemical features of the sympathetic component. Eur. J. Histochem. 57, 93-105.

Reimann W. and Schneider F. (1993). Galanin receptor activation attenuates norepinephrine release from rat spinal cord slices. Life Sci. 52, 251-254.

Shakova O and Sommer L. (2010). Neural crest-derived stem cells. In: The stem cell research community. Harvard Stem Institute. SteamBook, Cambridge.

Stewart A., Anderson R., Kobayashi K. and Young H. (2008). Effects of NGF, NT-3 and GDNF family members on neurite outgrowth and migration from pelvic ganglia from embryonic and newborn mice. BMC Dev. Biol. 8, 73.

Swindle M., Makin A., Herron A., Clubb J. and Frazier K. (2012). Swine as models in biomedical research and toxicology testing. Vet. Pathol. 49, 344-356.

Wanigasekara Y., Kepper M. and Keast J. (2003). Immunohistochemical characterisation of pelvic autonomic ganglia in male mice. Cell Tissue Res. 311, 175-185.

Wang X., Chan, A., Sham M., Burns A. and Chan W. (2011). Analysis of the sacral neural crest cell contribution to the hindgut enteric nervous system in the mouse embryo. Gastroenterology 141, 992-1002.

Wąsowicz K., Majewski M. and Łakomy M. (1998). Distribution of neurons innervating the uterus of the pig. J. Auton. Nerv. Syst. 74, 13-22.

Wąsowicz K., Podlasz P., Czaja K. and Łakomy M. (2002). Uterus-innervating neurones of paracervical ganglion in the pig: immunohistochemical characteristics. Folia Morphol. 61, 15-20.

Wiese C., Ireland S., Fleming N., Yu J., Valerius M., Georgas K., Chiu H., Brennan J., Armstrong J., Little M., McMahon A. and Southard-Smith E. (2012). A genome-wide screen to identify transcription factor expressed in pelvic ganglia of the lower urinary tract. Front. Neurosci. 6, 130.

Wiese C., Deal K., Ireland S., Cantrell V. and Sounthard-Smith E. (2017). Migration pathways of sacral neural crest during development of lower urogenital tract innervation. Dev. Biol. 429, 356-369.

Yan H. and Keast J.R. (2008). Neurturin regulates postnatal differentiation of parasympathetic pelvic ganglion neurons initial axonal projections, and maintenance of terminal fields in male urogenital organs. J. Comp. Neurol. 507, 1169-1183.

Yan H., Newgreen D. and Young H. (2003). Developmental changes in neurite outgrowth responses of dorsal root and sympathetic ganglia to GDNF, neurturin and artemin. Dev. Dyn. 227, 395-401.

Young H., Cane N. and Anderson C. (2011). Development of the autonomic nervous system: A comparative view. Auton. Neurosci. 165, 10-27.

Zalecki M. (2012). Localization and neurochemical characteristics of the extrinsic sympathetic neurons projecting to the pylorus in the domestic pig. J. Chem. Neuroanat. 43, 1-13.

Accepted December 3, 2020